# Dissection of the *Burkholderia* intracellular life cycle using a photothermal nanoblade

Christopher T. French[a], Isabelle J. Toesca[a], Ting-Hsiang Wu[b], Tara Teslaa[c], Shannon M. Beaty[a], Wayne Wong[a], Minghsun Liu[a], Imke Schröder[a], Pei-Yu Chiou[d,e], Michael A. Teitell[c,d,f,g,h], and Jeff F. Miller[a,d,h,1]

[a]Department of Microbiology, Immunology, and Molecular Genetics, [b]Department of Electrical Engineering, [c]Department of Pathology and Laboratory Medicine, [d]California NanoSystems Institute, [e]Department of Mechanical and Aerospace Engineering, [f]Broad Stem Cell Research Center, [g]Jonsson Cancer Center, and [h]Molecular Biology Institute, University of California, Los Angeles, CA 90095

Edited by Ralph R. Isberg, Tufts University School of Medicine, Boston, MA, and approved June 16, 2011 (received for review May 7, 2011)

***Burkholderia pseudomallei*** **and** ***Burkholderia thailandensis*** **are related pathogens that invade a variety of cell types, replicate in the cytoplasm, and spread to nearby cells. We have investigated temporal and spatial requirements for virulence determinants in the intracellular life cycle, using genetic dissection and photothermal nanoblade delivery, which allows efficient placement of bacterium-sized cargo into the cytoplasm of mammalian cells. The conserved Bsa type III secretion system ($T3SS_{Bsa}$) is dispensable for invasion, but is essential for escape from primary endosomes. By nanoblade delivery of *B. thailandensis* we demonstrate that all subsequent events in intercellular spread occur independently of $T3SS_{Bsa}$ activity. Although intracellular movement was essential for cell–cell spread by *B. pseudomallei* and *B. thailandensis*, neither BimA-mediated actin polymerization nor the formation of membrane protrusions containing bacteria was required for *B. thailandensis*. Surprisingly, the cryptic (*fla2*) flagellar system encoded on chromosome 2 of *B. thailandensis* supported rapid intracellular motility and efficient cell–cell spread. Plaque formation by both pathogens was dependent on the activity of a type VI secretion system (T6SS-1) that functions downstream from $T3SS_{Bsa}$-mediated endosome escape. A remarkable feature of *Burkholderia* is their ability to induce the formation of multinucleate giant cells (MNGCs) in multiple cell types. By infection and nanoblade delivery, we observed complete correspondence between mutant phenotypes in assays for cell fusion and plaque formation, and time-course studies showed that plaque formation represents MNGC death. Our data suggest that the primary means for intercellular spread involves cell fusion, as opposed to pseudopod engulfment and bacterial escape from double-membrane vacuoles.**

The robust Gram-negative bacillus *Burkholderia pseudomallei* (*Bp*) is endemic to warm, fecund soils of tropical regions (1, 2). Infections acquired from the environment can lead to melioidosis, a serious and sometimes fatal human disease. Accumulating evidence suggests that adaptations selected in the rhizosphere are responsible for "accidental virulence" in mammals (3). *Bp* has a large (7.2 Mb) genome that has been shaped by extensive horizontal exchange (4). *Burkholderia mallei* (*Bm*) is a clonal descendant of *Bp* that has undergone genome decay and has lost the capacity for environmental survival. *Bm* is the agent of equine glanders and it can also cause fatal human infections (2). Resistance to antibiotics and their low infectious dose have led to the classification of *Bp* and *Bm* as biowarfare threats.

The geographic distribution of *Bp* overlaps with that of *B. thailandensis* (*Bt*) and their genomes are highly similar and syntenic (5). Although *Bt* is rarely associated with human disease and is considered relatively nonpathogenic, this assessment is not absolute. Following aerosol challenge of mice, *Bt* causes fulminant, lethal infections that are dependent on virulence determinants shared with *Bp* and *Bm* (2, 6). *Bp*, *Bt*, and *Bm* invade and replicate in a wide range of cell types and exhibit nearly identical intracellular life cycles (1, 2). Following invasion and escape from endosomes, replication in the cytoplasm is accompanied by actin-based motility and cell–cell spread, analogous to *Shigella flexneri* and *Listeria monocytogenes* (7–9). Actin motility is mediated by BimA, a polarly localized surface protein that binds actin and promotes polymerization (9). An unusual feature of infection is the induction of cell fusion and the formation of multinucleate giant cells (MNGCs) (10). For *Bp* and *Bm* this requires BimA and has been observed with multiple cell types in vitro and in tissues from patients with melioidosis (2).

*Bp* possesses a generous endowment of specialized export systems including three "injection" type III secretion systems (T3SS), two of which are similar to those in phytopathogenic bacteria. The third, $T3SS_{Bsa}$, is homologous to the *Shigella* Mxi-Spa and *Salmonella* SPI-1 T3SSs and is highly conserved in *Bp*, *Bt*, and *Bm* (1, 2). $T3SS_{Bsa}$ is required for virulence in hamster and murine models of pathogenesis (2) and has been implicated in invasion of epithelial cells, escape from endosomes, intracellular survival, and evasion of autophagy (11). In addition, *Bp* encodes six type VI secretion systems (T6SSs) (12). Using the nomenclature of Schell et al. (13), T6SS-1 (also referred to as T6SS-5) (14) is critical for virulence in the *Bt* murine model of acute melioidosis and contributes to the lethality of *Bm* in hamsters (13). Recently, T6SS-1 mutants in *Bp* were shown to be capable of endosome escape in RAW264 cells but were defective in MNGC formation (15).

For intracellular pathogens, understanding the roles of virulence determinants is complicated by their involvement in temporally and spatially staged events. $T3SS_{Bsa}$ has been proposed to be required for late events associated with cell–cell spread, but direct investigation has been difficult since mutants are defective in earlier steps in the intracellular life cycle. To address this conundrum, we have used a photothermal nanoblade to deliver live bacteria directly into the cytoplasm of mammalian cells (16). The photothermal nanoblade device uses a laser pulse to excite a thin titanium coating on the tip of a glass capillary pipette. Rapid thermal excitation of the metallic nanostructure produces an explosive nanoscale vapor bubble that creates a small incision in the cell membrane at the point of pipette contact. This incision provides a transient delivery portal through which variably sized cargo—from molecules to bacteria—can be efficiently delivered with high cell viability. We have combined the use of this technology with traditional genetic ablation techniques and infection analysis to probe virulence mechanisms participating in the intracellular life cycle of *Burkholderia*.

Author contributions: C.T.F., I.J.T., and J.F.M. designed research; C.T.F., I.J.T., T.-H.W., T.T., S.M.B., and W.W. performed research; C.T.F., T.-H.W., P.-Y.C., M.A.T., and J.F.M. contributed new reagents/analytic tools; C.T.F., I.J.T., T.-H.W., T.T., S.M.B., M.L., I.S., and J.F.M. analyzed data; and C.T.F. and J.F.M. wrote the paper.

The authors declare no conflict of interest.

This article is a PNAS Direct Submission.

Freely available online through the PNAS open access option.

[1]To whom correspondence should be addressed. E-mail: jfmiller@ucla.edu.

This article contains supporting information online at www.pnas.org/lookup/suppl/doi:10.1073/pnas.1107183108/-/DCSupplemental.

## Results

**T3SS$_{Bsa}$ Is Required for Plaque Formation and Endosome Escape but Is Dispensable for Invasion.** HEK293 cells are efficiently invaded by *Bp* and *Bt* and are highly amenable to photothermal nanoblade-mediated cytosolic delivery. In the experiment in Fig. 1*A*, HEK293 monolayers were infected with *B. thailandensis* E264 (17), *B. pseudomallei* Bp340 (18), or derivatives containing in-frame deletions in *sctN*, which encodes the ATPase required for activity of the Bsa T3SS. Plaque formation, a hallmark of cell–cell spread, was eliminated in Δ*sctN* mutants and restored by complementation *in trans*. These observations are consistent with previous reports that plaque formation by *Bp* is dependent on T3SS$_{Bsa}$ (19).

It has been suggested that T3SS$_{Bsa}$ is required for invasion of nonphagocytic cells, a prerequisite for plaque formation (20). For Bp340 and BtE264, invasion was inhibited by cytochalasin D as expected, but it was unaffected by Δ*sctN* alleles (Fig. 1*B*). These results indicate that whereas invasion requires actin polymerization, it occurs independently of T3SS$_{Bsa}$ activity. Analogous results were obtained using HeLa cells (Fig. S1*A*). To determine whether T3SS$_{Bsa}$ facilitates endosome escape in HEK293 cells, monolayers were stained 8 h after infection for F-actin. As shown in Fig. S1*B*, BtE264 and Bp340 formed actin tails, indicating successful escape, whereas Δ*sctN* mutants and Δ*bimA* control strains did not. Moreover, Δ*sctN* mutants colocalized with the late endosomal marker LAMP1 (Fig. S1*C*). At later time points, only scattered bacterial debris was detected for Δ*sctN* mutants, suggesting they were killed and degraded due to endosomal entrapment (Fig. S1*D*). Although our results do not support a role for T3SS$_{Bsa}$ in invasion, they are consistent with previous reports of its essential contribution to endosome escape (2, 21).

**Intercellular Spread Following Cytoplasmic Delivery by a Photothermal Nanoblade.** The inability of Δ*sctN* mutants to escape from primary endosomes confounds efforts to understand the involvement of T3SS$_{Bsa}$ in subsequent steps required for cell–cell spread. Solutions to this dilemma require the ability to bypass early events that are otherwise essential during infection. To accomplish this, we exploited the capabilities of our recently developed photothermal nanoblade to place bacteria directly into the cytoplasm of host cells (Fig. 2*A*) (16). Because a nanoblade has not yet been customized and approved for use with *Bp* in a select agent BSL-3 facility, we focused our analysis on *Bt*, which can be safely manipulated under BSL-2 conditions.

In Fig. 2, wild-type (*WT*) BtE264 or mutant derivatives were introduced into HEK293 cells by infection or by photothermal nanoblade delivery. Plaque formation following infection was absolutely dependent on T3SS$_{Bsa}$ activity (Fig. 2*B*). When Δ*sctN* mutants were delivered into the cytosol using the nanoblade, they divided and polymerized actin as well as wild-type bacteria (Fig. 2*C*), demonstrating that actin motility functions independently of T3SS$_{Bsa}$ and does not require passage through the endosomal environment. We were surprised, however, to find that Δ*sctN* mutants were capable of forming plaques following nanoblade delivery that were indistinguishable in size and morphology from those formed by *WT Bt* following infection *or* nanoblade delivery (Fig. 2 *D*–*F*). The ability to bypass early events in the intracellular life cycle allows us to conclude that the *only* requirement for T3SS$_{Bsa}$ in cell–cell spread and plaque formation is for escape from primary endosomes following invasion. It had been assumed that for cell–cell spread to occur, T3SS$_{Bsa}$ would be required to lyse double-membrane secondary vacuoles formed during penetration of adjacent cells (1). Our observations indicate that either some other factor(s) performs this function, or intercellular spread occurs by an entirely different mechanism.

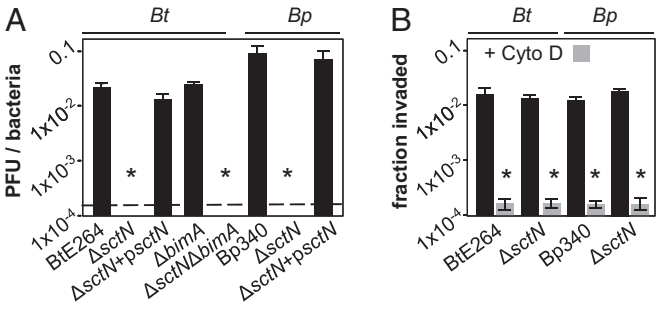


**Fig. 1.** T3SS$_{Bsa}$ is required for endosome escape but not invasion. (*A*) Plaque-forming units (pfu) per bacteria 18 h after infection of HEK293 cells with BtE264, Bp340, Δ*sctN* mutants, or complemented derivatives (p*sctN*). Dashed line, limit of detection. (*B*) Colony forming units (cfu) recovered per bacteria in 2-h invasion assays. HEK293 cells were untreated (solid bars) or treated with 2 μg/mL cytochalasin D (shaded bars) before infection. Assays were performed in triplicate and error bars represent ±SEM. *$P < 0.005$.

**Two Distinct Motility Systems Facilitate Plaque Formation.** A deletion mutant in *bimA* was included as a control for plaque formation in photothermal delivery experiments. As shown in Fig. S1*B* and Fig. 2*C*, the Δ*bimA* allele eliminates actin polymerization as previously described (22), and it also eliminates the formation of membrane protrusions containing *Burkholderia* at their tips. Although we assumed that actin motility would be required as a driving force for cell–cell spread, this notion was clearly incorrect. Following infection or nanoblade delivery, Δ*bimA* mutants formed plaques that were similar in size and morphology to those of their *WT* parent (Fig. 2 *B*, *D*, and *E*). BimA-mediated actin motility and the formation of membrane protrusions are therefore dispensable for cell–cell spread by *B. thailandensis*.

Intrigued by these results, we examined live infected cells by microscopy and discovered that *Bt* exhibits remarkably rapid intracellular motility. Bacteria move at speeds of >20 μm/s and often reverse course and change direction (Fig. S2*A* and Movies S1, S2, and S3). Because rapid intracellular motility was independent of BimA (Fig. 3*A*), we explored the possibility that flagellar motility was involved. Deletion of *motA1*, a motor component locus in the chromosome 1 flagellar biosynthesis gene cluster (*fla1*), eliminated swarming in soft agar but had no effect on intracellular motility or plaque formation (Fig. S2, Fig. 3 *A* and *B*, and Table S1). Previous studies identified potential chemotaxis and flagellar loci on chromosome 2 in *Bt* (23), and on closer inspection we found a full complement of flagellar structural and regulatory genes that could encode a second, functional motility system (*fla2*; Fig. S3). Deletion of *motA2* from the *fla2* flagellar cluster had no effect on swarming in agar or actin polymerization following invasion (Fig. S2*B* and Fig. 3*C*), but it eliminated rapid intracellular motility (Fig. 3*A*), as did deletion of *fliC2*, which is predicted to encode flagellin (Table S1). Although significant differences were not observed in plaquing efficiency (Fig. 3*B*), Δ*motA2* mutants formed plaques that were smaller than those produced by *WT* or Δ*bimA* strains (Fig. 3*D* and Table S1). When *motA2* was deleted from a Δ*bimA* background, plaque formation was almost completely abolished, and the defect was reversed by complementation with *motA2* (Fig. 3*B*).

These observations demonstrate that MotA2-dependent flagellar motility can drive intercellular spread independently of BimA-mediated actin polymerization, and at least one of the two motility systems must be active for plaque formation. Although flagellar motility does not affect invasion or endosome escape (Fig. 3*E* and Table S1), an interesting phenotype is observed in intracellular growth assays. As shown in Fig. 3*F*, *WT*, Δ*bimA*, and Δ*motA2* strains multiply, plateau at 12 h, and decrease in num-

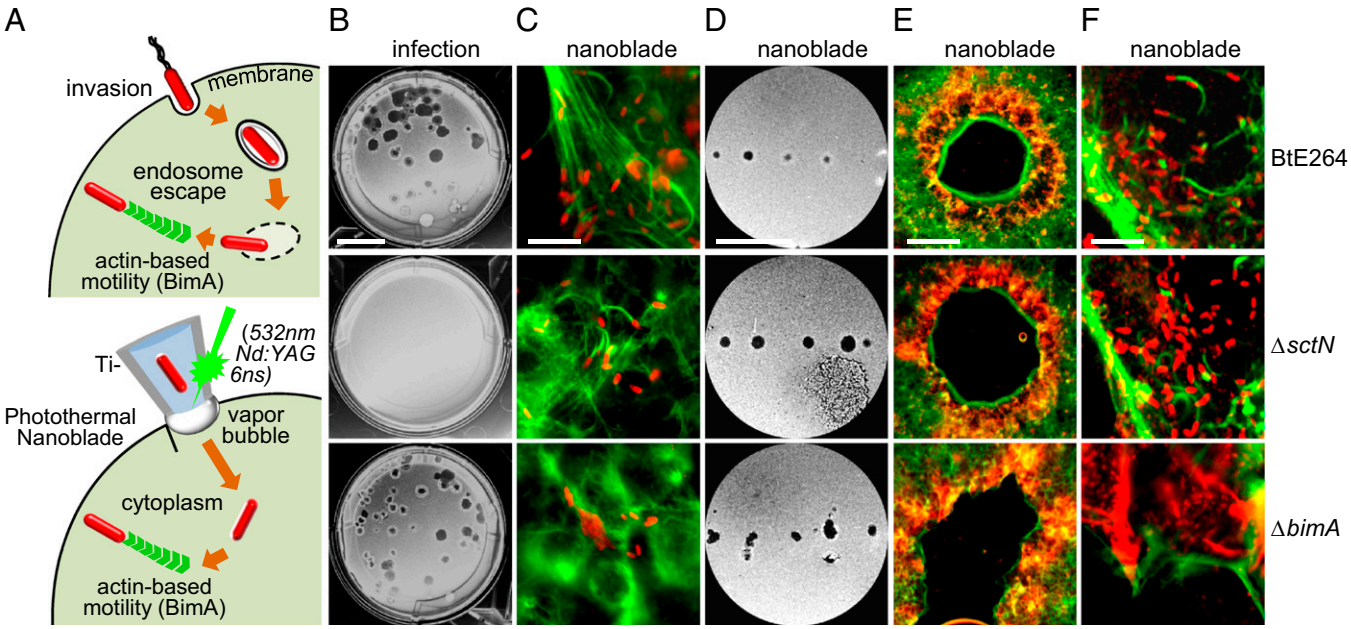


**Fig. 2.** Intercellular spread following photothermal nanoblade-mediated delivery. (*A*) *Upper*, invasion by BtE264 is followed by $T3SS_{Bsa}$-mediated endosome escape and BimA-mediated actin polymerization in the cytoplasm. *Lower*, photothermal excitation of Ti-coated microcapillary pipettes using a 6-ns, 532-nm laser pulse facilitates pressurized delivery of bacteria directly into the cytosol. (*B*) Plaque formation on HEK293 monolayers after infection with BtE264 (*Top*), Δ*sctN* (*Middle*), or Δ*bimA* mutants (*Bottom*). (Scale bar, 1 cm.) (*C*) *Bt* and mutants (red) were delivered into HEK293 cells using a photothermal nanoblade and stained for actin (green) 12 h later. (Scale bar, 20 μm.) (*D*) Plaque formation on HEK293 monolayers following nanoblade delivery. (Scale bar, 1 cm.) (*E*) Plaques in *D* stained for bacteria (red) and actin (green). (Scale bar, 500 μm.) (*F*) Magnified edges of plaques in *E*. (Scale bar, 20 μm.)

bers due to cell disruption and exposure to extracellular antibiotics. In contrast, Δ*bimA*Δ*motA2* mutants continue to multiply and reach significantly higher levels, suggesting a relationship between intracellular movement and cell death (see below).

**T6SS-1 Facilitates Plaque Formation.** Of the multiple T6SSs encoded by *Burkholderia* species, T6SS-1 has been repeatedly linked to host–pathogen interactions (12–15, 19). These correlations with virulence led us to investigate the role of T6SS-1 following infection and nanoblade delivery. T6SS-1 was inactivated by deletion of the *clpV1* ATPase (24). Δ*clpV1* mutants were fully invasive, escaped from endosomes, replicated in the cytoplasm, polymerized actin, and displayed rapid intracellular motility similar to *WT* (Fig. 4 *A*–*C*, Movie S3, and Table S1). In contrast, plaque formation following infection (Fig. 4*D*) or nanoblade delivery (Table S1) was reduced to near background levels, demonstrating that *clpV1*-dependent T6SS activity is crucial for intercellular spread.

Motility and T6SS-1 mutants exhibited similar phenotypes. In both cases major defects in plaque formation are observed, and as shown in Fig. 4*C*, Δ*clpV1* mutants replicate to higher numbers in intracellular growth assays, similar to the Δ*bimA*Δ*motA2* double mutant (Fig. 3*F*). As shown in Fig. 4*E*, the kinetics of cell death are significantly delayed following infection by Δ*clpV1* mutants, suggesting that increased bacterial numbers reflect prolonged cell survival. In considering how these and earlier observations might be related, a closer look at the process of plaque formation itself is revealing.

**Intercellular Spread and Plaque Formation Occur Through Cell Fusion.** *Bp*, *Bm*, and *Bt* induce cell fusion and multinucleate giant cell (MNGC) formation with remarkable efficiency in a variety of cell types (2, 10, 25). In observing cell monolayers following nanoblade delivery, we often noticed the appearance of MNGCs in areas that developed to become plaques. To examine the process more closely, we constructed HEK293 cell lines that constitutively express green fluorescent protein (GFP) or monomeric strawberry red fluorescent protein (RFP) by stable transduction with recombinant lentivirus. In Fig. 5*A*, GFP- and RFP-expressing cells were seeded at a 1:1 ratio and *Bt* or mutant derivatives were introduced by infection or nanoblade delivery. The progression of events leading to plaque formation is readily apparent; individual cells (red or green) initially fuse to form one or more MNGCs (yellow), which later lyse to form a clear zone in the monolayer surrounded by a ring of fused cells (i.e., a plaque). A MNGC containing numerous DAPI-stained nuclei before lysis is shown in Fig. 5*B*.

Fig. 5*C* shows early (12 h, *Upper*) and late (24 h, *Lower*) time points in cell fusion-plaque assays with BtE264 or mutant strains. Although Δ*sctN* mutants failed to form MNGCs or plaques following infection due to endosomal entrapment, both events occurred normally after nanoblade delivery, demonstrating that $T3SS_{Bsa}$ is not required for MNGC formation. In BtE264, deletion of *bimA* or *motA2* individually had little effect, whereas a Δ*bimA*Δ*motA2* double mutant was greatly delayed in MNGC formation. A similar phenotype was observed with the Δ*clpV1* strain. A Δ*sctN*Δ*clpV1* mutant was incapable of MNGC formation following infection, but resembled the Δ*clpV1* single mutant after nanoblade delivery, showing that T6SS-1 affects cell–cell spread downstream of $T3SS_{Bsa}$-mediated endosomal escape (Fig. 5*C* and Table S1). Fig. 5*D* shows that plaque formation by *B. pseudomallei* also occurs through a process that involves MNGC formation and lysis and is dependent on *clpV1*. Because Bp340 lacks *fla2* (Fig. S3 and *Discussion*), this process required *bimA*. On the basis of these and other results, we propose that cell fusion is the central mechanism for cell–cell spread by *B. thailandensis* and *B. pseudomallei* and that plaque formation occurs through a process that is dependent on the formation of MNGCs. This result differs fundamentally from intercellular spread by *Listeria monocytogenes*, which requires actin-based motility, engulfment of bacterial protrusions by adjacent cells, and escape from double-membrane vacuoles (8). Indeed, as shown in Fig. 5*E*, plaque formation by *Listeria* occurs in the absence of detectable cell fusion.

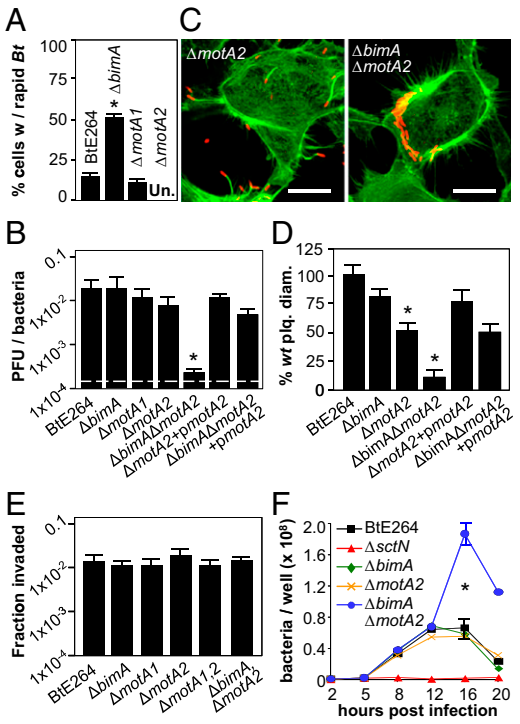


**Fig. 3.** *fla2*-mediated flagellar motility facilitates plaque formation. (*A*) Fraction of HEK293 cells containing rapidly motile bacteria 8 h after infection with BtE264 and derivatives. Approximately 300 cells were monitored per strain. (*B*) Plaque-forming efficiency on HEK293 cell monolayers 18 h after infection. (*C*) Representative infected cells stained for bacteria (red) and actin (green). (*D*) Plaque diameters 24 h after infection of HEK293 cell monolayers. (*E*) HEK293 cell invasion efficiencies by BtE264 or mutant strains 2 h postinfection. (*F*) Time course of intracellular replication in HEK293 cells. All assays were performed in triplicate and error bars represent ±SEM. $*P < 0.005$; Un, undetectable.

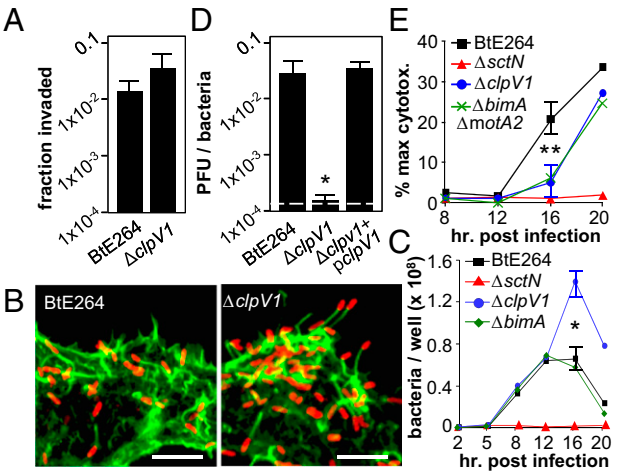


**Fig. 4.** T6SS-1 is critical for efficient intercellular spread. (*A*) Invasion efficiencies by BtE264 or Δ*clpV1* mutants 2 h postinfection in HEK293 cells. (*B*) HEK293 cells were infected and stained for bacteria (red) and actin (green) 8 h postinfection. (Scale bar, 20 μm.) (*C*) Time course of intracellular replication in HEK293 cells. (*D*) Plaque-forming efficiency on HEK293 cell monolayers 18 h after infection. (*E*) Cytotoxicity assays in HEK293 cells. All assays in *A* and *C*–*E* were performed in triplicate and error bars represent ±SEM. $**P < 0.05$; $*P < 0.005$.

## Discussion

Our results are incorporated into a model for the *Burkholderia* intracellular life cycle shown in Fig. S4. This model is based on observations with HEK293 cells and may not take into account factors that are specifically required for survival and replication in professional phagocytes.

**Invasion.** Invasion of HEK293 cells by *Bp* or *Bt* requires host-cell actin polymerization but not the activity of $T3SS_{Bsa}$, contrasting with a clear requirement for the Mxi-Spa and SPI-1 T3SSs in invasion by *Shigella* (7) and *Salmonella* (26), respectively, and with expectations for *Burkholderia* based on analyses of BopE, a $T3SS_{Bsa}$ substrate homologous to *Salmonella* SopE and SopE2 (20). In an experiment often cited as supporting a role for $T3SS_{Bsa}$ in invasion (20), insertion mutations in *bipD* (a $T3SS_{Bsa}$ translocon gene) or *bopE* conferred modest decreases in invasion (35–40%) 6 h after infection of HeLa cells. The discrepancy between these data and ours is likely due to the use of a late time point where endosomally trapped mutants loose viability (6 h in ref. 20 vs. 2 h in Fig. 1), giving the appearance of an invasion defect. A similar conclusion was previously reported by Haraga et al., using BtE264 and HeLa cells (21). Their study and ours support the conclusion that for *Bp* and *Bt*, invasion of nonphagocytic cells can occur by mechanisms that are independent of $T3SS_{Bsa}$. Virulence determinants that mediate invasion await discovery.

**Bsa T3SS.** $T3SS_{Bsa}$ is required for escape from endosomes following invasion of HEK293 cells by *Bp* or *Bt*, consistent with numerous prior studies with a variety of cell types (1, 2). Cytosolic delivery of *Bt* using a photothermal nanoblade allowed us to bypass endosome escape and directly examine the role of $T3SS_{Bsa}$ in downstream events: actin polymerization, cell–cell spread, and MNGC formation. In all cases the results were remarkably clear; plaque formation following infection was absolutely dependent on $T3SS_{Bsa}$, whereas plaque formation following nanoblade delivery was independent of its activity. The same was true for MNGC formation. We also show that replication and actin polymerization occur normally when Δ*sctN* mutants are placed directly into the cytosol.

These observations have several implications; first, they allow us to conclude that in our system, the *only* role for $T3SS_{Bsa}$ is to facilitate escape from primary endosomes of initially infected cells. Next, our results help explain a perplexing lack of phenotypes associated with known or putative effectors. In contrast to obvious requirements for the Bsa T3SS in vitro and in vivo (2), to our knowledge no effectors have been *definitively* shown to be required for invasion, replication in nonphagocytic cells, cell–cell spread, MNGC formation, or virulence in animals. BopA, a suspected $T3SS_{Bsa}$ substrate, is reported to facilitate survival and evasion of autophagy in phagocytic cells (11), but *bopA* mutants are not significantly attenuated in mice (2). The precise mechanism of T3SS-mediated endosome escape is unknown for any intracellular pathogen; however, it could conceivably be a function of translocon insertion in the endosomal membrane and occur in the absence of additional effectors. Finally, there is an instructive contrast between the roles of the *Burkholderia* Bsa and *Shigella* Mxi-Spa T3SSs. The *Shigella* system is essential for both endosome escape and escape from double-membrane vacuoles formed during the process of cell–cell spread (7). For *Burkholderia*, our results support a model for intracellular spread that obviates the need for membrane lysis after the primary endosome has been breached.

**Intracellular Motility.** Polarized, unidirectional actin polymerization is a hallmark of cell–cell spread and plays an essential role for *Shigella*, *Listeria*, and other intracellular pathogens (9). The discovery that *Bt* remains fully capable of plaque formation in the absence of BimA was quite unexpected. Even more sur-

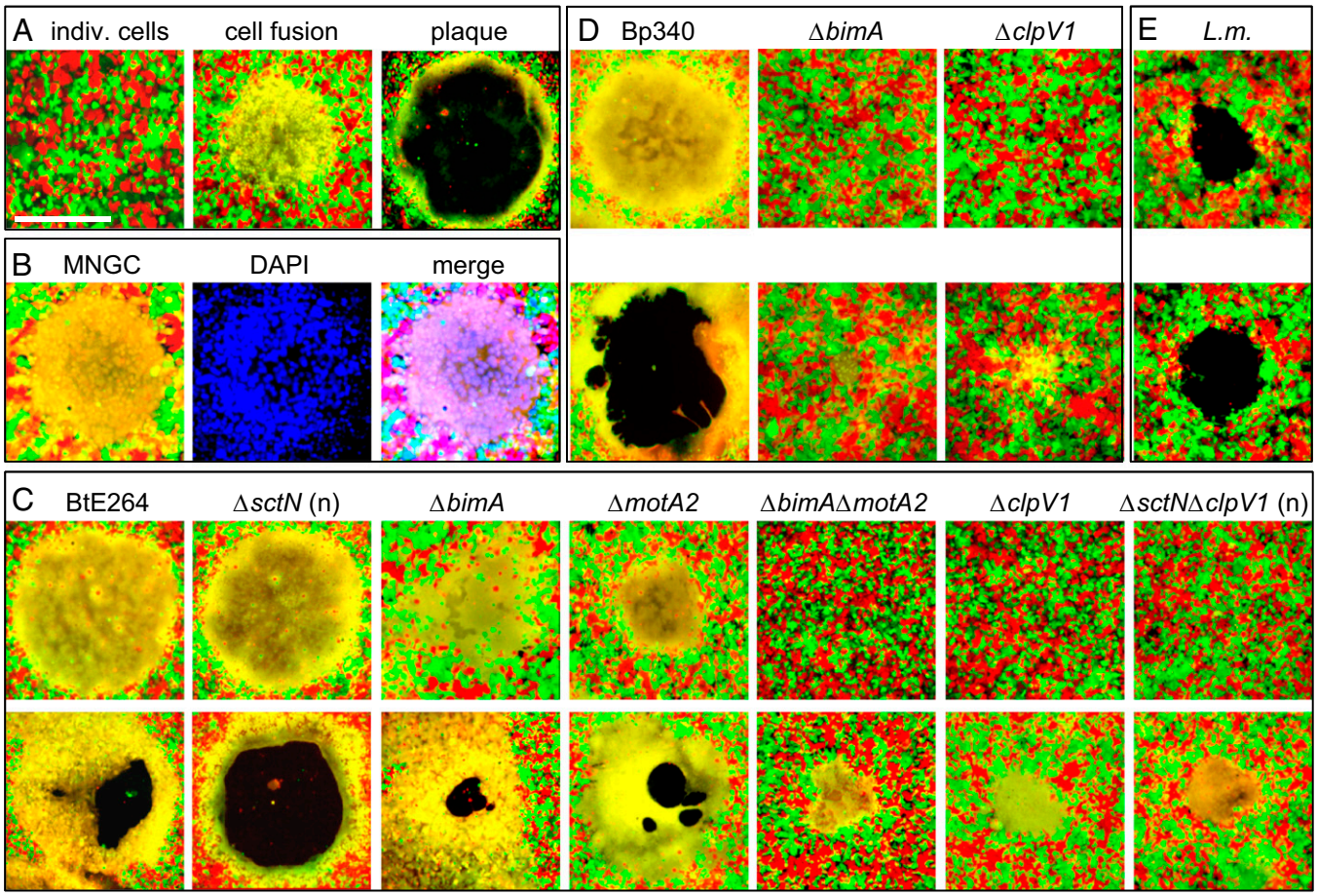


**Fig. 5.** Intercellular spread and plaque formation occur through cell fusion. (*A*) Progression of events leading to plaque formation. (*Left*) HEK293-RFP (red) and -GFP (green) cells immediately after infection. Twelve hours later, a MNGC is formed (yellow, *Center*), which undergoes lysis and forms a plaque at 24 h (*Right*). (Scale bar, 500 μm.) (*B*) A MNGC (*Left*) was stained with DAPI (blue, *Center*). (*Right*) Triple-color merged image. (*C*) MNGC and plaque formation by BtE264 and mutants on HEK293 RFP + GFP monolayers 12 h (*Upper*) or 24 h (*Lower*) following infection or nanoblade delivery ("n", Δ*sctN*, Δ*sctN*Δ*clpV1*). (*D*) MNGC and plaque formation 12 h (*Upper*) and 24 h (*Lower*) after infection with Bp340 and mutants. (*E*) Plaque formation 56 h following infection with *L. monocytogenes* 10403S. The slight appearance of yellow at the edge of plaques is due to physical overlap of red and green cells and does not indicate cell fusion. Images are representative of multiple independent experiments.

prising was the observation that a predicted flagellar system on chromosome 2 (*fla2*) can compensate for the lack of actin motility and drive intercellular spread and MNGC formation.

The *Bt* and *Bp fla1* flagellar gene clusters on chromosome 1 are highly conserved. *fla1* encodes polar flagella, which in *Bp* have been implicated in invasion of epithelial cells and virulence in animal models (2). In *Bt*, mutation of *motA1* (*fla1*) or *motA2* (*fla2*) individually or in combination had no effect on invasion. Although this is a first characterization of dual flagellar motility systems in an intracellular pathogen, their occurrence and functions have been described in *Vibrio* and *Aeromonas* spp., where they facilitate motility in response to different environmental signals (27). Not surprisingly, *fla1* and *fla2* in *Bt* were observed to function under different conditions; deletion of *motA1* eliminated swarming in soft agar but had no effect on motility following infection. Conversely, deletion of *motA2* had no effect in soft agar but eliminated rapid intracellular motility.

Our sequence analysis suggests that *fla2* encodes lateral flagella (Fig. S3*B*), but this prediction awaits direct confirmation. It is also unknown how the system is regulated or whether intracellular bacteria are simultaneously capable of BimA-mediated actin polymerization and *fla2*-dependent motility. Because flagellin monomers are known to activate assembly of the NLRC4 inflammasome, resulting in cytokine production and inflammatory cell death (28), the use of flagella for intra- and intercellular motility is surprising. It is presently unknown whether *fla2* flagellin induces inflammasome-dependent cytoplasmic responses or whether mechanisms to overcome them exist. Perhaps the most important question involves the relevance of our observations with *Bt* to pathogenesis in *Bp* and *Bm*. A recent analysis of the global population structure of *Burkholderia* species pathogenic for mammals predicts an Australian origin for *Bp*, with a single introduction event leading to the expansion of Southeast Asian isolates (SEA *Bp*) and *Bm* (29). Interestingly, the *fla2* gene cluster is absent in SEA *Bp* isolates such as Bp340, which is dependent on BimA for plaque formation (Fig. 5*D*), but it is highly conserved in sequenced genomes from Australian strains (Fig. S3) (23). The potential role of the *fla2* locus in pathogenesis by Australian *Bp* remains to be investigated.

**T6SS-1.** T6SSs are widely distributed among pathogenic and nonpathogenic Gram-negative species; they have broad roles in survival and fitness and have been linked to virulence in numerous pathogens, including *Bp*, *Bm*, and *Bt* (2, 14). In our analysis, T6SS-1 was found to facilitate intercellular spread following infection or photothermal delivery. Consistent with recent reports (14, 15, 19), deletion of *clpV1* resulted in a defect in plaque formation in HEK293 cells and a delay in the formation

of MNGCs. Δ*clpV1* mutants exhibited robust actin-polymerization and flagellar-mediated motility inside cells, and genetic dissection using the photothermal nanoblade established that T6SS-1 functions downstream of invasion and $T3SS_{Bsa}$-mediated endosome escape. Concomitant with decreased efficiency of MNGC formation, we observed an increase in cell survival following infection with Δ*clpV1* mutants and an accumulation of intracellular bacteria. These data are consistent with the hypothesis that T6SS-1 participates in events that can alternatively facilitate intercellular spread by fusing cell membranes or kill cells by compromising their integrity.

**Cell Fusion and Intercellular Spread.** *Burkholderia* efficiently induce MNGC formation in both phagocytic and nonphagocytic cells (10). We propose that cell fusion represents the primary path for intercellular spread and plaque formation by *Bt* and *Bp* (Fig. S4), and the same is likely to hold true for *Bm*. These observations are consistent with the results of time course experiments showing that the formation of MNGCs and their eventual lysis give rise to the open cores of plaques, and with the lack of a requirement for $T3SS_{Bsa}$ in cell–cell spread following cytosolic delivery of bacteria using our photothermal nanoblade. Whereas *Bt* $T3SS_{Bsa}$ mutants are incapable of endosome escape following infection, *Bp* $T3SS_{Bsa}$ mutants are reported to exhibit delayed escape that eventually leads to MNGC formation (30), consistent with our proposal that cell–cell spread occurs independently of $T3SS_{Bsa}$ activity for both *Bt* and *Bp*. Furthermore, mutations that eliminate intracellular motility or inactivate T6SS-1 have analogous effects on MNGC formation and cell–cell spread following photothermal delivery or infection. Our model also explains the lack of published reports demonstrating double-membrane vacuoles following engulfment of protrusions with *Burkholderia* at their tips, as observed with *L. monocytogenes*, *S. flexneri*, and other pathogens with similar lifestyles (7, 8). Although membrane protrusions are readily formed by wild-type *Bt*, they are not observed with Δ*bimA* mutants. The ability of Δ*bimA* strains that retain *fla2* motility to efficiently form plaques shows that membrane protrusions are not required for intercellular spread.

Our results, along with a recent report from Stevens et al. (22), demonstrate a clear link between motility and the efficiency of cell fusion by intracellular *Burkholderia*. We hypothesize that flagellar and/or actin-mediated motility increases the frequency of contact between bacteria and host cell membranes and that contact is prerequisite for membrane fusion through a process facilitated by T6SS-1. It is tempting to speculate that a bacterially encoded fusogenic factor is involved in this unique mechanism of cell–cell spread.

## Materials and Methods

Detailed experimental procedures are found in *SI Materials and Methods*. BtE264 (17) and Bp340 (SEA *Bp* 1026b Δ*amrRAB-oprA*) (18) mutants were constructed using allelic exchange as described (31). Nanoblade delivery was performed as described in *SI Materials and Methods* and in ref. 16.

**ACKNOWLEDGMENTS.** We thank the University of California (Los Angeles) Vector Core for lentiviral reagents and Mary Burtnick at the University of South Alabama for *Bt* antiserum. This work was supported by the Pacific Southwest Regional Center of Excellence in Biodefense and Emerging Infectious Diseases (U54 A1065359) (to J.F.M.), the National Science Foundation [Chemical, Bioengineering, Environmental, and Transport Systems (CBET) 0853500 and Electrical, Communications, and Cyber Systems (ECCS) 0901154] (to P.-Y.C.), a University of California Discovery Biotechnology Award (178517) (to P.-Y.C.), the National Institutes of Health Roadmap for Medical Research Nanomedicine Initiative (PN2EY018228) (to M.A.T.), and an Innovator Award from the Broad Stem Cell Research Center at University of California, Los Angeles (to M.A.T.). C.T.F. is supported by a National Institutes of Health Ruth L. Kirschstein National Research Service Award (GM07185), the Warsaw Microbiology Fellowship, and the University of California (Los Angeles) Dissertation Fellowship.

1. Wiersinga WJ, van der Poll T, White NJ, Day NP, Peacock SJ (2006) Melioidosis: Insights into the pathogenicity of Burkholderia pseudomallei. *Nat Rev Microbiol* 4:272–282.
2. Galyov EE, Brett PJ, DeShazer D (2010) Molecular insights into Burkholderia pseudomallei and Burkholderia mallei pathogenesis. *Annu Rev Microbiol* 64:495–517.
3. Nandi T, et al. (2010) A genomic survey of positive selection in Burkholderia pseudomallei provides insights into the evolution of accidental virulence. *PLoS Pathog* 6: e1000845.
4. Holden MT, et al. (2004) Genomic plasticity of the causative agent of melioidosis, Burkholderia pseudomallei. *Proc Natl Acad Sci USA* 101:14240–14245.
5. Kim HS, et al. (2005) Bacterial genome adaptation to niches: Divergence of the potential virulence genes in three Burkholderia species of different survival strategies. *BMC Genomics* 6:174.
6. West TE, Frevert CW, Liggitt HD, Skerrett SJ (2008) Inhalation of Burkholderia thailandensis results in lethal necrotizing pneumonia in mice: A surrogate model for pneumonic melioidosis. *Trans R Soc Trop Med Hyg* 102(Suppl 1):S119–S126.
7. Ray K, Marteyn B, Sansonetti PJ, Tang CM (2009) Life on the inside: The intracellular lifestyle of cytosolic bacteria. *Nat Rev Microbiol* 7:333–340.
8. Tilney LG, Portnoy DA (1989) Actin filaments and the growth, movement, and spread of the intracellular bacterial parasite, Listeria monocytogenes. *J Cell Biol* 109: 1597–1608.
9. Stevens JM, Galyov EE, Stevens MP (2006) Actin-dependent movement of bacterial pathogens. *Nat Rev Microbiol* 4:91–101.
10. Kespichayawattana W, Rattanachetkul S, Wanun T, Utaisincharoen P, Sirisinha S (2000) Burkholderia pseudomallei induces cell fusion and actin-associated membrane protrusion: A possible mechanism for cell-to-cell spreading. *Infect Immun* 68: 5377–5384.
11. Gong L, et al. (2011) The Burkholderia pseudomallei type III secretion system and BopA are required for evasion of LC3-associated phagocytosis. *PLoS ONE* 6:e17852.
12. Pukatzki S, et al. (2006) Identification of a conserved bacterial protein secretion system in Vibrio cholerae using the Dictyostelium host model system. *Proc Natl Acad Sci USA* 103:1528–1533.
13. Schell MA, et al. (2007) Type VI secretion is a major virulence determinant in Burkholderia mallei. *Mol Microbiol* 64:1466–1485.
14. Schwarz S, et al. (2010) Burkholderia type VI secretion systems have distinct roles in eukaryotic and bacterial cell interactions. *PLoS Pathog* 6:e1001068:.
15. Burtnick MN, et al. (2011) The cluster 1 type VI secretion system is a major virulence determinant in Burkholderia pseudomallei. *Infect Immun* 79:1512–1525.
16. Wu TH, et al. (2011) Photothermal nanoblade for large cargo delivery into mammalian cells. *Anal Chem* 83:1321–1327.
17. Brett PJ, DeShazer D, Woods DE (1998) Burkholderia thailandensis sp. nov., a Burkholderia pseudomallei-like species. *Int J Syst Bacteriol* 48:317–320.
18. Mima T, Schweizer HP (2010) The BpeAB-OprB efflux pump of Burkholderia pseudomallei 1026b does not play a role in quorum sensing, virulence factor production, or extrusion of aminoglycosides but is a broad-spectrum drug efflux system. *Antimicrob Agents Chemother* 54:3113–3120.
19. Pilatz S, et al. (2006) Identification of Burkholderia pseudomallei genes required for the intracellular life cycle and in vivo virulence. *Infect Immun* 74:3576–3586.
20. Stevens MP, et al. (2003) A Burkholderia pseudomallei type III secreted protein, BopE, facilitates bacterial invasion of epithelial cells and exhibits guanine nucleotide exchange factor activity. *J Bacteriol* 185:4992–4996.
21. Haraga A, West TE, Brittnacher MJ, Skerrett SJ, Miller SI (2008) Burkholderia thailandensis as a model system for the study of the virulence-associated type III secretion system of Burkholderia pseudomallei. *Infect Immun* 76:5402–5411.
22. Sitthidet C, et al. (2010) Actin-based motility of Burkholderia thailandensis requires a central acidic domain of BimA that recruits and activates the cellular Arp2/3 complex. *J Bacteriol* 192:5249–5252.
23. Tuanyok A, et al. (2007) A horizontal gene transfer event defines two distinct groups within Burkholderia pseudomallei that have dissimilar geographic distributions. *J Bacteriol* 189:9044–9049.
24. Shalom G, Shaw JG, Thomas MS (2007) In vivo expression technology identifies a type VI secretion system locus in Burkholderia pseudomallei that is induced upon invasion of macrophages. *Microbiology* 153:2689–2699.
25. Boddey JA, et al. (2007) The bacterial gene lfpA influences the potent induction of calcitonin receptor and osteoclast-related genes in Burkholderia pseudomallei-induced TRAP-positive multinucleated giant cells. *Cell Microbiol* 9:514–531.
26. Patel JC, Galán JE (2005) Manipulation of the host actin cytoskeleton by Salmonella—all in the name of entry. *Curr Opin Microbiol* 8:10–15.
27. McCarter LL (2004) Dual flagellar systems enable motility under different circumstances. *J Mol Microbiol Biotechnol* 7:18–29.
28. Miao EA, et al. (2010) Caspase-1-induced pyroptosis is an innate immune effector mechanism against intracellular bacteria. *Nat Immunol* 11:1136–1142.
29. Pearson T, et al. (2009) Phylogeographic reconstruction of a bacterial species with high levels of lateral gene transfer. *BMC Biol* 7:78.
30. Burtnick MN, et al. (2008) Burkholderia pseudomallei type III secretion system mutants exhibit delayed vacuolar escape phenotypes in RAW 264.7 murine macrophages. *Infect Immun* 76:2991–3000.
31. Barrett AR, et al. (2008) Genetic tools for allelic replacement in Burkholderia species. *Appl Environ Microbiol* 74:4498–4508.